UC Berkeley
Technical Completion Reports

Title

Climate Variability of the Sierra Nevada Over the Last Millennium: Reconstructions from Annually Laminated Sediments in Swamp Lake, Yosemite National Park, CA

Permalink

https://escholarship.org/uc/item/7kg3c1vg

Authors

Cayan, Daniel R
Charles, Christopher D

Publication Date

2010-03-01

Project Title: Climate Variability of the Sierra Nevada Over the Last Millennium: Reconstructions from Annually Laminated Sediments in Swamp Lake, Yosemite National Park, CA.

Principle Investigators:
Daniel Cayan, Scripps Institution of Oceanography, University of California San Diego
dcayan@ucsd.edu
Christopher Charles, Scripps Institution of Oceanography, University of California San Diego ccharles@ucsd.edu

Abstract

Persistent drought presents one of the greatest risks of climate change faced by the western United States. Highlighting this risk is from paleo hydrological evidence that during the medieval period (~900-1400 AD) this region experienced two extensive droughts of greater duration than any experienced in recorded history. However, much remains to be learned about these "mega droughts," including the severity of deficit in precipitation and snowpack in California's Sierra Nevada Mountain range, which currently serve as a crucial source of fresh water to California agriculture, industry and domestic users. To possibly extract a record of the hydrological conditions in the Sierra Nevada during this era, cores of annually laminated sediment from Swamp Lake, in the northwest portion of Yosemite Park were collected. Stable hydrogen isotope (δD) ratios of plant leaf-wax lipid compounds preserved in the lake sediments and the thickness of the annual sedimentary laminations (varves) show promise as potential proxies for recording past hydroclimate variability in the Sierra Nevada Mountains. δD measurements at annual to interannual resolution were made for two time periods: the 20th century and the 13th-15th centuries while varve thickness was measured over the entire period 1150-2006 AD. We find significant negative correlations between 20th century δD fluctuations and instrumentally recorded variability in total precipitation, snow water equivalence (SWE) and Palmer Drought Severity Index (PDSI). Medieval δD values correspond to independent regional hydrologic reconstructions at the decadal to multi-decadal scale, which appear to delineate relatively dry medieval episodes. An issue that is still unclear is that the mean δD during this period is little different from that during the relatively moist contemporaneous period. This finding is at odds with evidence from submerged tree stumps for two prolonged droughts separated by about 200 years. Varve thickness measurements are on going, but results thus far reveal difficulties in using this proxy for reconstructing past Sierra Nevada hydroclimate variability, the most significant being the complexity of the seasonal deposition cycle and sub-millimeter thicknesses. Overall, geochemical and geomorphological information gleaned from Swamp Lake sediment cores provide an independent means of reconstructing hydroclimate in the Sierra Nevada and provide a unique perspective on the mega-drought intervals in the Sierra Nevada Mountains.

Introduction

Assessing the risks of persistent drought in the western United States requires multiple realizations of decadal and centennial scale hydrologic variability that extend beyond the relatively short period of instrumental record. Of particular interest is the hydrologic evolution of the Sierra Nevada Mountains in central California. The majority total annual precipitation in these mountains arrives in the frontal passage of wintertime (November-March) storms (Markham 1970). As it melts in the spring and summer, the snowpack deposited during these storms serves as a crucial source of year-round fresh water, accounting for 40% of the water supply to urban and agricultural centers in southern and central California after April 1 (Roos 1989). Alpine snowpack storage is

highly sensitive to climate warming, and may already be responding in lower catchments, which in recent decades have exhibited an increasing fraction of precipitation falling as rain and less as snowfall (Knowles et al. 2006), advances in spring snowmelt-driven runoff (Roos, 1991; Dettinger & Cayan, 1994; Cayan et al. 2001; Regonda et al. 2005; Stewart et al. 2005), and a diminished accumulation of spring snowpack (Mote et al 2005; Howat and Tulaczyk 2005). While numerical simulations project an envelope of future conditions, full assessment of drought risk over the coming decades also requires an understanding of past variability extending beyond the period of historical observation.

Evidence unearthed from a variety of paleoclimate archives including tree rings (Cook *et al*., 1999, 2004), lake sediments (Woodhouse & Overpeck, 2000) and drowned tree stumps (Stine, 1994) indicates that throughout the western United States hydrologic conditions were drier on average during the early part of the last millennium (900-1400 AD) than those of historical record. These archives also capture the occurrence during this time of several so-called "mega-droughts," periods of protracted aridity sustained for multiple decades that were of equal or greater severity than historical droughts (Stine, 1994; Cook *et al*., 1999, 2004; Woodhouse & Overpeck 1998; Herweijer *et al*., 2007; Seager *et al*., 2008). The first evidence for these droughts was reported by Stine (1994) in the form of relict tree stumps submerged in Tenaya Lake and several other present-day water bodies in central California. The radiocarbon dates of the outermost ring on these stumps, or "death dates," fall in two groups, one set around 1100 AD and another around 1350 AD. The presence of these stumps suggests that water levels were low enough for periods of time sufficient to foster the growth of mature pine trees. Cook *et al*. (1999) expanded upon this evidence using a gridded network of tree ring width chronologies spanning much of the western United States to reconstruct hydroclimate at annual resolution over the last millennium. Exploiting the sensitivity of several tree species to water supply, the authors use statistical techniques and a modern calibration to quantitatively convert tree-ring thicknesses into PDSI values. Having updated the network with additional chronologies, Cook *et al*. (2004) present the Drought Area Index (DAI), a time series documenting the percentage of grid squares in a given year experiencing drought conditions, as indicated by a reconstructed PDSI value < -2 (Figure 1). This DAI record reveals four "mega-droughts" in the western United States centered on 936, 1034, 1150 and 1253 AD (Cook *et al*., 2004) (Figure 2).

While the extensive Palmer Drought Severity Index (PDSI) reconstruction of Cook *et al*. (2004) provides a large-scale view of drought evolution over the last millennium, PDSI is known to be problematic as a index of hydrologic conditions in mountainous areas were water supply is dominated by snow melt (Hayes, 2006). Depending on their local setting, trees may be good at recording dry conditions but not wet, or vice-versa. Furthermore, tree-reconstructed PDSI from Cook *et al*., 2004 incorporate tree-ring chronologies from a relatively broad area, and therefore no one grid square is targeted towards variability in the Sierra Nevada Mountains.

Lacustrine sedimentary records provide an excellent alternative archive for climate information that can be extracted through geochemical and morphological analyses. This information is particularly well preserved when seasonal overturning fails to ventilate the bottom of the water column (meromictic conditions), prohibiting bioturbating macrofuana from disturbing the seasonally deposited sedimentary layers and allowing the formation of varves, which furnish an environmental "clock" of annual resolution. Varved lacustrine sediment cores have been used in countless paleoclimate

investigations from all over the United States and the world. Studies from high latitudes lakes in Canada indicate that varve thickness can serve as a proxy for stream discharge in locations where peak runoff is dominated by spring and summer snowmelt, such as Yosemite National Park (Forbes & Lamoureux, 2005; Lamoureux *et al*., 2006, Menounos *et al*, 2005). These studies further demonstrate that in such locations, the sediment load transported during this nival peak is highly correlated with SWE: large SWE generating higher volume runoff capable of carrying an elevated load. For example, Lamoureux *et al*. (2006) use varved sediments from a lake in the Canadian middle arctic to expose a decline in spring discharge since the mid 17th century due to a decrease in snowpack and thus SWE over this time. Varve records are particularly well suited for resolving interannual climate change and can even be used to identify stochastic events of hydrological significance such as single rainstorm induced floods (Menounos *et al*., 2005) or glacial discharges such as those from the Agassiz Ice Cap described by Sheldon *et al*. (2004).

Hydrogen isotope ratios (δD) of specific plant lipid compounds preserved in lake sediments offer an additional means to independently reconstruct hydroclimate. Long chain leaf wax lipids from terrestrial and aquatic plants are refractory compounds that remain well preserved in lacustrine sediments (Meyers & Ishiwatari 1993) even for millions of years (Yang & Huang, 2003). At ambient temperatures the carbon bound lipid hydrogens do not exchange with the surrounding environment (Schimmelman *et al*., 1999) and thus retain their δD value through time. Environmental water (precipitation, surface water and shallow ground water) is the only source of hydrogen for plant lipid biosynthesis. The δD of these reservoirs is controlled by climate parameters such as temperature, evaporation, moisture source and storm track (Craig, 1961; Dansgaard, 1964; Ehhalt *et al*., 1963; Friedman *et al*., 1964; Gat 1996). At midlatitudes the δD of precipitation is primarily determined by the fraction of original vapor that remains in the air mass when precipitation occurs and the fraction of that moisture that gets recycled back to the atmosphere through evapotranspiration (Ingraham & Taylor 1986, 1991). The moisture in land-falling frontal storms of north Pacific origin becomes progressively depleted in deuterium as the storms move inland due to the preferential loss, under equilibrium conditions, of deuterium (D or ^2H) over protium (^1H) from the vapor to the denser phase (water or snow). The highly non-linear relationship between temperature and water's saturation vapor pressure coupled with adiabatic cooling that occurs as the air mass travels east and rises over the Sierra Nevada crest results in a sharp δD gradient with values decreasing ~35-40‰ per 1000m elevation gain along the western slope of the mountain range (Friedman & Smith 1970; Smith *et al*., 1979; Ingraham & Taylor, 1991). The precipitation along this slope is therefore depleted in deuterium by ~60-180‰ relative to the ocean water from which the moisture derived.

The temperature at which moisture first evaporates and later condenses also contributes to meteoric δD composition. Fractionation between the vapor and water phases increases with decreasing temperature (Majzoub, 1971). The initial vapor in equilibrium with water at 10ºC will be depleted by ~18‰ compared that in equilibrium with water at 25ºC. Conversely, precipitation condensing at colder temperatures will have elevated δD values due to enhanced fractionation between the vapor and the denser phases. Evaporation off the surface of rain drops and snow that melts prior to deposition shifts δD towards heavier values as the heavier isotope becomes concentrated in the liquid phase. Partial or total requilibration with moisture at lower elevations and warmer

temperatures can also increase the δD value of rain drops that formed higher up in the atmosphere (Friedman *et al*., 1962, 1964). Due to slow rates of isotopic exchange between ice and vapor, snowflakes are not subject to these processes and preserve their original δD values as they fall.

Post-depositional processes will further influence the δD composition of environmental water. In a study of precipitation, surface water and shallow ground waters along three zonal transects across California and Nevada Ingraham & Taylor (1991) document the increasing contribution of evapotranspiration to moisture recycling and the δD value of precipitation, surface water and shallow ground water with increasing distance inland. This recycling causes a weakening of the δD versus distance gradient as it deviates from that expected in a completely open system where all precipitation is removed through runoff. Using a simplified water balance model, the authors calculate upwind recycling by evapotranspiration contributes 22% of environmental water at the Sierra Nevada crest. Evapotranspiritive processes at the catchment scale impart a further isotopic influence on hydrogen of surface and shallow ground waters ultimately utilized in plant metabolism. Evaporation of soil moisture and off lake surfaces can have a disproportionately large isotopic enriching effect on these reservoirs despite limited overall contribution to the catchment's water budget (Kendall & McDonnell, 1998). Leydecker and Melack (2000) reveal that annual average evaporation (including transpirative processes) accounts for ~36% of annual precipitation in high elevation catchments in the western Sierra Nevada Mountains. Catchment scale evapotranspiration therefore has the potential to significantly impact δD of environmental water prior to its use in plant lipid biosynthesis.

The incorporation of environmental water into plant lipid compounds results in a biological fractionation due primarily to the biochemical discrimination of deuterium in lipid biosynthesis but also due to biophysical processes that act on leaf water, most importantly the enriching effects of evapotranspiration in terrestrial and emergent aquatic plants. Current studies suggest that this fractionation primarily determined by the metabolic pathway or biosynthetic precursor, in other words, it is not a function of environmental factors such as temperature (Sessions, 1999). In agreement with this observation, plant lipid δD has been shown to track δD of environmental water across numerous climatic gradients. Sauer *et al*. (2001) find a direct correlation between δD of algal and terrestrial lipids from lake surface sediments to the overlying lake water along a latitudinal gradient in the northeast United States and southern Canada. Similar studies by Sachse *et al*. (2004, 2006) and Huang *et al*. (2004) along a N/S transect of European and North American lakes respectively shows that sedimentary n-alkanes of terrestrial and aquatic origins also track their source lake water. Hou *et al*. (2008) compare δD of sedimentary terrestrial leaf wax n-acids to δD of precipitation and lake water across an expansive humidity, annual precipitation and vegetative gradient in the American southwest. The authors find a significant correlation between lipid δD, and that of the source environmental waters.

These empirical studies suggest that plant lipid δD can capture that of environmental water with fidelity and therefore capture temporal variability in the physical climate mechanisms that drive meteoric δD fluctuations. Down core sedimentary records of aquatic and terrestrial plant lipid δD in the American northeast have been shown to reflect millennial scale climate amelioration during the most recent deglaciation recorded in the GISP2 ice cores d18O as well and local pollen temperature

reconstructions (Huang *et al*., 2002, 2006). However, plant lipid δD has yet to be employed for interannual to decadal scale reconstructions, in part due to that difficulty in isolating sufficient concentrations of lipid compounds for isotopic analysis. However, in numerous locations such as the Sierra Nevada Mountains where the absence of carbonate precipitation in lakes prohibits the use of more conventional paleo-hydrologic isotopic techniques, lipid δD serves as the sole means to capture isotopic variability of meteoric water, a key tool for reconstructing past hydrologic conditions.

       The organic rich, annually laminated (varved) sediments of Swamp Lake offer the ideal archive from which to measure leaf wax lipid δD variability at interannual resolution. Here we measure the δD of four leaf wax n-acids extracted from a suite of sediment cores collected from Swamp Lake. Measurements were made over two periods, the 20th century and the 12th-15th centuries. We have three main objectives for this study: 1) use comparisons with instrumental climate records to assess the fidelity with which leaf wax lipid δD and varve thickness captures Sierra Nevada climate variability 2) distinguish the physical mechanisms responsible for driving observed δD and varve thickness variability and 3) use down-core δD and varve thickness measurements and conclusions drawn from 20th century comparisons to reconstruct Sierra Nevada hydroclimate at decadal scales and test the hypotheses that conditions of severe aridity prevailed in the drainage basin surrounding Swamp Lake during the medieval period.

Methods

Study Site and Field Sampling

       Swamp Lake is located at the northwest corner of Yosemite National Park (37º57'N, 119º46'W, 1554 m elevation), on the western side of the Sierra Nevada crest (Figure 2). The lake, a flat, relatively deep (~ 20 m) basin surrounded by steep sides and a surface area of about 0.6 hectares, sits in an isolated catchment with an area of 1.6 hectares over granite bedrock with a single seasonal inlet and no distinct outlet, but rather, a broad swampy overflow at the west end and, presumably, groundwater seepage. Protected within the confines of one of the country's oldest National Parks, Swamp Lake has received negligible human impact, its sediment input undisturbed throughout the Holocene. Temperatures at Swamp Lake fluctuate above and below freezing between December and March indicating that the catchment receives a mixture of rain and snow during winter storms. The meteorological station at Hetch Hetchy reservoir, located approximately 2 miles east and 370 m below Swamp Lake, receives an annual average of 35 inches precipitation, Total precipitation, however, varies considerably from year to year, with values between 50% and 200% of climatological averages not uncommon (Lundquist *et al*. 2005).

       Lake surface temperatures reach 4ºC in December and begin to rise again at the end of March, suggesting that the lake is dimictic or remains well mixed throughout the winter. However, any mixing related oxygenation of the lake depocenter is too short to support bioturbating macrofuana, as evidenced by the continual presence of varves in sediments spanning the last millennium. Oxygen and temperature profiles from July 2009

(figure 2b) reveal the presence of an established summer thermocline between 5-6 m and dysoxia at depth. The lake is mesotrophic, supporting an abundant planktonic diatom community and numerous aquatic macrophytes in the shallow regions.

Sediment cores were collected during field expeditions to Swamp Lake in the falls of 2006 and 2007. In order to preserve the uppermost sedimentary layers deposited over the 20th century, we employed the freeze coring technique, which entails freezing a sedimentary crust ~1.5 cm thick onto a hollow, weighted, aluminum wedge filled with a dry ice-ethanol slurry. The resulting frozen sedimentary wedge is then removed and stored in a cooler with solid CO_2 until storage in the permanent -20ºC freezer facility at the Scripps Institution of Oceanography (SIO). We also used a Boliva corer, a more conventional device better suited for capturing longer cores and thus older material. Bolivia cores were transported out of the field at room temperature and later stored in a 4ºC refrigerator at SIO. In total we extracted 8 freeze cores and 6 Bolivia cores.

Water and vegetation samples were collected during a third field expedition in July 2009. Water samples were collected from the center of Swamp Lake at the surface, 2m, 4m, 5m, 6m, 8m, 10m, 12m and 14m depth and stored in 50 mL HDPE bottles sealed with parafilm to hinder evaporation, capped and wrapped in aluminum foil to prevent exposure to light. Temperature and dissolved oxygen concentrations were measured at the same depths at which water was sampled. The resulting temperature vs. depth profile reveals a well-developed thermocline between 5-6 m with surface water temperatures of ~25ºC falling to ~5ºC sub-thermocline. Difficulties with reading stability on the oxygen meter reduced the number of usable dissolved oxygen measurements. Table 1 lists the species, type and location of 16 vegetation samples from Swamp Lake and its surroundings catchment. Samples consisting of several leaves and short stem pieces were placed in Ziploc bags and transported frozen in a cooler containing dry ice. They were later stored at -20ºC at the Scripps Institution of Oceanography. Sub-samples were lyophilized prior to analysis.

In 2006 a Solinst level logger (Lundquist 2003) and an Onset TIDBITS air temperature logger were installed at the west end of the lake and hung from a nearby tree respectively. These instruments were retrieved and replaced annually through July 2009.

Core Logging and Imaging

All freeze cores and 5 of 6 Bolivia cores were logged at the Limnological Research Center at the University of Minnesota, Minneapolis (LRC) in the months following each expedition. In addition to basic core processing, high-resolution digital images of core surfaces were taken at the LRC using DMT CoreScan (at 100 pixels per cm resolution) and Geotek GeoScan-III (at 200 pixels per cm resolution) digital linescan cameras. Also at the LRC, subsamples of frozen sediment cores were embedded with Spurr's low viscosity epoxy resin and smear slides were taken along various depths in the Boliva cores for microscopic inspection. Once cured, embedded subsamples were cut on a rock saw and sent to San Diego Petrographic in Emmett ID where thin sections were made.

Determination of Chronology

The age-depth chronology for the 20th century was compiled by repeated counting of laminated couplets on high resolution digital images of freeze core surfaces following predetermined criteria for defining varves such that a year was counted only if a light band was clearly present. Clear marker bands were identified on the suite of cores to allow for visual correlation and assessment of varve counting error. Inspection of a massive unit at ~25cm depth reveals grading of sediment from course sand and small pebbles on the bottom to a fine clay cap at the top, suggesting that this section was formed from a bank failure rather than oxygenation of the lake bottom waters. Furthermore, on all cores counted, the clay cap fell within ten varve years of 1872, the date of the powerful Owens Valley earthquake, which was documented to have been strongly felt in Yosemite Valley by John Muir himself and to have generated a similar slump in Owens Lake (Li *et al*. 2000). Spectral analysis of grey scale values from the 20th century core section results in a peak at the one year frequency band, confirming the presence of annual laminations. Finally, microscopic inspection of thin sections confirms that varve couplets consist of seasonally alternating layers of diatom frustules (summer/fall) and terrigenous organic matter often including charcoal (winter/spring).

The medieval chronology remains preliminary pending the results of tephra analysis. However, a preliminary chronology was developed assuming the shallowest tephra layer originated from the 1350 Inyo Craters eruption (Millar *et al*., 2006). Assuming a constant sedimentation rate, we interpolated between this tephra layer and the bottom the slump assumed to be 1872. The resulting sedimentation rate of 0.6 mm/yr agrees with a second sediment rate independently determined from varve counting down from the bottom of the slump to the shallowest tephra layer.

Varve Thickness Measurement and Image Analysis

Varve thickness analyses were conducting using the MATLAB software package. Freeze core images were linearly translating images from the RGB to the CIE L*a*b* color space following the procedure outlined by Nederbragt *et al*. (2004). The L channel of the Lab color scheme more closely resembles the human eye's perception of lightness than grey scale RGB or CMYK and it is thus better suited for image analysis of sedimentary surfaces. Vertical linescan grey scale curves were generated by averaging L (light/dark) values over a column 50 pixels wide. The inflection points of the second derivative of this curve correspond to the transition from light and dark between varve components. Existing software packages employ this method to distinguish annual banding in tree rings (e.g. DendroScan) and corals (e.g. CoralXDS). However, unique properties of Swamp Lake varve morphology necessitate a customized approach involving a number of image processing and mathematical steps. Briefly, the zeroes of the second derivative of a down core grey scale curve are calculated. Each zero corresponds to the transition between light and dark. The pixels corresponding to each zero are converted to core depth, allowing for the measurement of varve thickness in mm.

Water Sample δD analysis

Stable isotope ratios (δD and δ^{18}O) of Swamp Lake water samples were measured in the lab of Alex Sessions at the California Institute of Technology in Pasadena, CA on a Los Gatos Research Liquid Water Analyzer 908-0008 following the instrument set up described in detail in Lis *et al.* (2008). Four measurement cycles were carried out with five injections per measurement. A standard of known δD and d18O, -59‰ and -8.5‰ VSMOW respectively, measured after every four unknowns, was used to in order to determine unknown isotopic values of Swamp Lake water samples. An additional sample of known isotopic value, LGR3, was analyzed in every cycle and treated as an unknown to evaluate measurement accuracy. The average standard deviation for δD and d18O measurements was 0.7‰ and 0.2‰ respectively.

Sediment and Vegetation Sample Preparation and Lipid Identification

All processing and analysis of sediment samples was carried out in the lab of Alex Sessions at the California Institute of Technology in Pasadena, CA. Frozen sediment cores were sampled in a -20ºC cold box with a razor blade. 20th century sediments were sampled at annual to interannual resolution at selected core depth based on chronology. The down core interval for each sample ranged from 2-5mm. Medieval sediments were sampled at 2 mm intervals in the same manner. Samples were placed into precombusted 20mL glass vials and lyophilized. Lyophilized samples were weighed, with masses ranging from 0.01-0.53g, and solvent-soluble lipids extracted in 20mL of the 9:1 dimethyl chloride: methanol azeotrope in a Mars Express microwave-assisted solvent-extraction system (Mars 5, CEM corp.) for 30 min at 100ºC with stirring. Vegetation sub-samples were placed in precombusted 20mL glass vials, lyophilized, and cut into approximately 1 cm x 1 cm pieces with solvent cleaned scissors. The solvent-soluble total lipid extract (TLE) by was extracted by sonicating in DCM for two 10 minute intervals.

Sediment and vegetation TLEs from all but one species (*A. viscida*) were separated into four organic fractions: alkanes, ketones, alcohols and fatty acids using solid phase extraction (SPE) procedure described in Sessions *et al.* (1999) and Sessions (2006). The fatty-acid fraction was derivatized as methyl esters by refluxing with boron trifluoride in methanol at 70ºC for 1 hr. The resulting fatty acid methyl esters (FAMEs) were analyzed on a ThermoFinnigan Trace GC-DSQ quadrupole mass spectrometer equipped with a DB-5 column (30 m x 0.25 mm x 0.25µm) and PTV injector operated in splitless mode. The relative abundance of even carbon number FAMES C20-C32 was determined by integrating peak area.

δD Analysis of Vegetation and Sediment Samples

δD analyses of individual FAMEs was carried out on a ThermoElectron Trace GC coupled to a Delta + XP IRMS via an Al2O3 pyrolysis chamber. All measurements took

place in the lab of Alex Sessions at the California Institute of Technology in Pasadena, CA. δD values were determined relative to at least two peaks of methane reference gas (C.P. grade) of δD of -148‰ and reported relative to VSMOW in per mil units. To correct for H_3^+ interference with mass-3 (Sessions *et al*., 2001a, 2001b), the H_3^+ factor was calculated daily by measuring the mass 3/2 signal ratio of 10 peaks of H_2 reference gas (δD = -150‰) with varying peak intensities covering the range of most H_2 peaks from analyzed sample compounds. No internal standard was injected due to lack of space within noisy sample chromatograms, but an external standard containing 8 n-alkanes (F8) of known δD value determined independently offline was analyzed at the start and finish of every sample run and between every two to four samples to assess measurement accuracy, with the average absolute offset of 3.13‰ (N=75). The average difference between duplicate measurements of medieval samples was 4.6‰, 3.8‰, 3.4‰, 2.3‰ and (N= 70, 69, 69, 70) for sediment FAMEs C22, C24, C26, C28 and vegetation FAME C24 respectively.

Results

Lake Water δD, Temperature and Dissolved O2 Profiles

Swamp Lake July 2009 water column δD values begin at ~-78‰ at the surface and 2m depth, and increase between 4 and 8m depth to -75‰ where they remain to 14m, the deepest depth sampled (Figure 3a). The transition from relatively light to heavier values roughly corresponds to the depth of the thermocline (Figure 3b). There is a distinct dissolved oxygen maximum at 4m, likely the base of the epilimnion, deeper than which dissolved oxygen steadily declines to ~7mg/L (Figure 3b). Measurements were not made deeper than 14m, but a water sample brought up from the bottom in September 2007 smelled of hydrogen sulfide, indicative of anoxic conditions at the lake bottom.

Vegetation n-acid Distribution

Relative distributions of n-acids C20-C32 were measured for 15 vegetation species ranging from submerged aquatic plants to hardwoods. Although n-acid distributions of aquatic and terrestrial plants do not show distinct differences, aquatic plants tend to have higher relative abundances of the shorter chain n-acids C20-C24 than the higher order terrestrial plants, as evidenced by averaging the distributions of the two plant sets (Figure 4). The C20-C32 n-acid distribution of sediment samples showed little change with depth with C24 being the most abundant compound in all samples, the few exceptions being samples with a double maximum at C24 and C26. The typical sediment distribution more closely resembles that of the submerged, floating and emergent plants than it does the grasses, shrubs and trees.

20th Century Sediment δD

The δD of even number n-acids C22-C28 was measured in 72 Swamp Lake sediment samples spanning 1898-2006. The range of variability over this interval is ~50‰ ranging from -185‰ to -135‰ and variability is shared among the four compounds (Figure 5). The average δD value of all compounds is -167‰ with a standard deviation of 14‰. A clear multi-decadal signal is present in the 20th century record. The δD time series from C24, which has the highest sedimentary abundance of the four n-acids measured in this study, is the most complete owing to the consistently large C24 peak intensity and area. We therefore chose this record to compare with instrumental climate records.

In Figure 8 the 20th century C24 time series is compared to total annual precipitation from Hetch Hetchy Reservoir and California Climate Division 5, which covers the San Joaquin drainage basin, April 1 snow water content (SWC) from Bee Hive Meadows (BHV) and Donner Summit (DNS), and three records of PDSI, two instrumental and one reconstructed from nearby tree ring chronologies by Cook *et al*., 2008. All climate records are smoothed with a two year running mean to mimic the smooth inherent in the sediment record and interannual sampling resolution. Table 2 lists the correlation coefficients of the 20th century C24 time series with this set of modern climate records. C24 δD variability is negatively correlated with all hydrologic indices, such that lower (more negative) δD values correspond to instrumental observations of wetter conditions. While all correlations are significant at the 95% confidence interval, the strongest is that with BHV SWE.

The strength of this relationship let us to investigate further the connection between the amount of snowpack remaining at the end of the winter and the δD value recorded by sedimentary leaf wax n-acids. We assigned a single year to each sample using our varve chronology and the core depths incorporated. Figure 8 shows the correlation between the C24 δD record and April 1 SWE anomalies at California Department of Water Resources (CDWR) and National Resources Conservation Service (NCRS) SNOTEL snow courses throughout the western United States (D. Pierce, personal communication). With only a few exceptions, April 1 SWE anomaly at every station is negatively correlated with the δD record, with about half the correlations signification at the 95% confidence interval. We then divided 20th century C24 δD values into quartiles and composited the April 1 SWE anomalies from Sierra Nevada snow courses for the years corresponding to δD values falling below the 1st and above the 3rd quartile, the lowest 25% and highest 25% of the data set which we refer to as low δD and high δD respectively. Positive SWE anomalies throughout the Sierra Nevada for the low δD year composite and while negative SWE anomalies prevail for the high δD year composite, again reinforcing the connection between low (high) δD values and elevated (diminished) snowpack.

Finally, we composited the dates of spring pulse timing, in other words the timing of peak snowmelt as recorded in the hydrograph, from a collection of Sierra Nevada river gauges (M. Dettinger, personal communication) for the low δD and high δD years. Stream flow records are from the USGS Hydro-Climate Data Network (HCDN), a dataset containing observations from rivers and river basins with little anthropogenic influence on their natural flow (Slack & Landwehr 1992). Only gauges missing less than 14 years (~25%) of data between 1948 and 2006 were analyzed. We subtracted the spring pulse

timings of the low δD year composite from the high δD year composite and that on average the pulse timing from the low δD group arrived 10 days later in the spring than for the high δD group, with longer delays at some stations.

Medieval Sediment δD

The even numbered C22-C28 n-acid δD of a total of 89 samples spanning the time period 1150 to 1450 AD were measured (Figure 6). δD variability is on the order of 30‰ with values ranging from -195‰ to -155‰. Average δD from all compounds is -175‰ with a standard deviation of 7‰. Data show significant decadal scale variability on the order of 30‰, which is shared among the four n-acids measured.

In order to determine whether decadal scale fluctuations reflect hydroclimate variability, we compares the δD time series of the four compounds to the gridded tree ring width PDSI reconstructions from the North American Drought Atlas (NADA) (Cook *et al*., 2008; Cook & Krusic, 2004). Figure 7 shows the comparison of the C24 δD record with a PDSI reconstruction from the most proximal 2.5° x 2.5° grid square in the NADA. The δD record reflects decadal scale PDSI fluctuations, but does not capture the lower frequency centennial scale changes in hydroclimate recorded in the tree ring record.

Conclusions

An assessment of the major findings of this study at this stage remains preliminary as analysis and interpretation of all data sets is ongoing. We cannot draw conclusions based on the varve thickness measurements at this time. However, with the δD data at hand we can being to draw conclusions about 1) the fidelity with which δD of long chain n-acids preserved in Swamp Lake sediment capture hydrologic variability, 2) the physical climate mechanisms responsible for driving observed δD fluctuations, 3) hydrologic conditions in the Sierra Nevada Mountains during the second of two western US-wide mega droughts.

Correspondence between δD values and both instrumental hydroclimate records and tree ring PDSI reconstructions indicate that leaf wax lipid δD variability does record aspects of climate variability in the Sierra Nevada Mountains. The correlation with April 1 SWE anomalies is the most robust of the suite of records analyzed, suggesting that the amount of snow that remains in the Sierra Nevada at the end of the winter influences the δD values recorded by plant leaf wax lipids during the following growing season. Due to the relatively low elevation of Swamp Lake, the relationship with April 1 SWE records may reflect that amount of moisture that is released the to the Swamp Lake catchment in the late winter and early spring just prior to the start of the growing season. Winters with heavy precipitation, reflected by large April 1 snowpacks, result in the flushing of the Swamp Lake catchment with isotopically depleted water deposited during wintertime North Pacific storms. The heavier moisture pulse to the basin delays the onset of peak evaporation until later in the growing season (Leydecker & Melack 2000) and through volume considerations limits the mass balance isotopic enrichment effects of

evapotranspiration. Less flushing of the basin occurs following winters of lower precipitation, allowing a greater relative proportion of existing water, which was subject to evaporation during the previous summer, available for uptake by plants. Furthermore, peak evaporation occurs earlier in the growing season and has a greater mass balance isotopic influence, which is subsequently recorded in elevated δD values of plant leaf wax lipids. Comparisons of the Swamp Lake δD profile measured in 2009 with those of another researcher, Joseph Street at Stanford University in Palo Alto, CA, reveal that lake surface water can vary by as much as 20‰ over the course of the growing season, ranging from low δD values in the spring to elevated δD values in the late summer. However, the timing of this shift from lower, presumably snow-melt driven values to higher, evaporation driven values can vary from summer to summer. During summers following winters of heavier precipitation, particularly those with abundant late winter and spring precipitation, lake surface waters and shallow ground waters in the Swamp Lake catchment will remain depleted in δD longer into the growing season.

However, the observed δD variability could be influenced by factors such as moisture source and storm track, which can result in interannual δD variability of precipitation (ref) that would then be recorded in plant lipids. Further analysis is necessary to complete our determination of the driving mechanisms responsible for the δD observations over the 20th and the medieval period. Without having fully identified these mechanisms, it is difficult to interpret the medieval δD time series in terms of the hydrologic conditions that prevailed in the Sierra Nevada during the period 1150-1450 AD. Nevertheless, we can enumerate the following major findings of this study this far: 1) The δD of long chain leaf wax lipids in Swamp Lake exhibit variability on interannual to decadal scales that appears to be influenced in part by climatological fluctuations, specifically the amount of wintertime precipitation that is delivered to the lake basin 2) The isotopic influence of evaporation of lake surface water and shallow ground water during the growing season, controlled by the amount of winter and early spring moisture in the basin, may be the dominant control of the δD value recorded by leaf wax lipids 3) Medieval δD variability reveals decadal scale hydroclimate variability also reflected in independent regional hydroclimate reconstructions. The absence of low frequency, centennial scale variability in this δD record may reflect the fact that leaf wax hydrogen isotopes record different climatological signals than other proxies typically used to reconstruct hydrologic conditions. Overall, these results provide an independent means of investigating hydroclimate variability in the Sierra Nevada over the last millennium. The Medieval δD record allows us to assess the climatological processes involved in the mega droughts, information that will aid in the anticipation and mitigation of further droughts.

References

Barnes, C. J. and J. V. Turner, 1998. *Isotopic exchange in soil water.* in Isotope Tracers in Catchment Hydrology. Kendall C. and J. J. McDonnell eds. Elsevier 137-162.

Cayan, D.R., S.A. Kammerdiener, M.D. Dettinger, J.M. Caprio, and D.H. Peterson, 2001: Changes in the Onset of Spring in the Western United States. Bull. Am. Met. Soc., **82**, 399-415

Cook, E. R., *et al.*, 2004. Long-term aridity changes in the western United States. *Science* **306**, 1015-1018.

Cook, E. R., *et al*., 1999. Drought reconstructions for the continental United States. *Journal of Climate* **12**, 1145-1162.

Cook, E. R., *et al*., 2008. North American Summer PDSI Reconstructions, Version 2a. IGBP PAGES/World Data Center for Paleoclimatology Data Contribution Series # 2008-046. NOAA/NGDC Paleoclimatology Program, Boulder CO, USA. http://www.ncdc.noaa.gov/paleo/pdsi08_ts.html

Cook, E.R. and P.J. Krusic. 2004. The North American Drought Atlas. Lamont-Doherty Earth Observatory and the National Science Foundation. http://iridl.ldeo.columbia.edu/SOURCES/.LDEO/.TRL/.NADA2004/.pdsi-atlas.html

Craig, H., 1961. Isotopic variations in meteoric waters. *Science* **133** 1702-1703.

Dansgaard, W., 1964. Stable isotopes in precipitation. *Tellus* **16** 436-468.

Dettinger, M. D., and Cayan, D. R., 1994. Large-Scale Atmospheric Forcing of Recent Trends toward Early Snowmelt Runoff in California. *Journal of Climate* **8**, 606-622.

Ehhalt, D. *et al*., 1963. Deuterium and oxygen-18 in rain water. *Journal Geophysical Research* **68**, 3774-3780.

Forbes, C. A. and Lamoureux, S. F., 2005. Climatic Controls on Stream flow and Suspended Sediment Transport in Three Large Middle Arctic Catchments, Boothia Peninsula, Nunavut, Canada. *Arctic, Antarctic and Alpine Research* **37**, 304-315

Friedman I. *et al*., 1962. Water vapor exchange between a water droplet and its environment. *Journal of Geophysical Research* **67**, 2761-2766.

Friedman I. *et al*., 1964. The Variation of the Deuterium Content of Natural Waters in the Hydrologic Cycle. *Reviews of Geophysics* **2**, 177-224.

Friedman, I. and G. I. Smith, 1970. Deuterium content of snow cores from the Sierra Nevada area. *Science* **169**, 467-470.

Gat, J. R., 1996. Oxygen and hydrogen in the hydrologic cycle. *Annual Review of Earth and Planetary Sciences* **24**, 225-262.

Hayes, M. J., Drought Indices. National Drought Mitigation Center. www.drought.unl.edu/whatis/indices.htm#pdsi, 2006. Accessed June 1, 2006.

Herweijer, C., *et al*., 2007. North American droughts of the last millennium from a gridded network of tree-ring data. *Journal of Climate* **20**, 1353-1376.

Hou, J. *et al*., 2008. Can sedimentary leaf waxes record D/H ratios of continental precipitation? Field, model and experimental assessments. *Geochimica et Cosmochimica Acta* **72**, 3503-3517.

Howat, I. M., and S. Tulaczyk (2005), Climate sensitivity of spring snowpack in the Sierra Nevada, *J. Geophys. Res.*, *110*, F04021, doi:10.1029/2005JF000356

Huang, J. H. *et al*., 2002. Hydrogen isotope ratios of palmitic acid in lacustrine sediments record late Quaternary climate variations. *Geology* **30**, 1103-1106.

Huang, J.H. *et al*., 2004. Hydrogen isotope ratios of individual lipids in lake sediments as novel tracers of climatic and environmental change: A surface sediment test. *Journal of Paleolimnology* **31**, 363-375.

Huang, J. H. *et al*., 2006. Postglacial climate reconstruction based on compound-specific D/H ratios of fatty acids from Blood Pond, New England. *Geochemistry Geophysics Geosystems*. **7**(3), doi: 10.1029/2005GC001076.

Ingraham, N. L. and B. E. Taylor, 1986. Hydrogen isotope study of large-scale meteoric water transport in northern California and Nevada. *Journal of Hydrology* **85**, 183-197.

Ingraham, N. L. and B. E. Taylor, 1991. Light stable isotope systematics of large-scale hydrologic regimes in California and Nevada. *Water Resources Research* **27**, 77-90.

Knowles, N., *et al*., 2006. Trends in snowfall versus rainfall in the western United States. *Journal of Climate* **19**, 4545-4559.

Leydecker, A. and J. M. Melack, 2000. Estimating evaporation in seasonally snow-covered catchments in the Sierra Nevada, California. *Journal of Hydrology* **236**, 121-138.

Lis, G. *et al*., 2008. High-precision laser spectroscopy D/H and 18O/16O measurements of microliter natural water samples. *Analytical Chemistry* **80**, 287-293.

Lundquist, J. D., Cayan, D. R., and Dettinger, M. D., 2003. Meteorology and hydrology in Yosemite National Park: A Sensor Network Application, in *Information Processing in Sensor Networks: Second International Workshop, IPSN 2003* (F. Zhao and L. Guibas eds), 518-528, Springer, New York.

Lundquist, J. D., Dettinger, M. D., and Cayan, D. R., 2005. Snow-fed Stream flow Timing at Different Basin Scales: Case Study of the Tuolumne River above Hetch Hetchy, Yosemite, California. *Water Resources Research* **41** W07005.

Majzoub, M., 1971. Fractionnement en oxygene-18 et en deuterium entre l'eau et sa vapeur. *Journal of Chemical Physics* **68**, 1423-1436.

Markham, C. G., 1970. Seasonality of Precipitation in the United States. *Annals of the Association of American Geographers* **60,** 593-597.

Menounos, B. *et al*., 2005. Environmental reconstruction from a varve network in the southern Coast Mountains, British Columbia, Canada. *The Holocene* **15**, 1163-1171.

Meyers, P. A. and R. Ishiwatari, 1993. Lacustrine organic geochemistry—An overview of indicators of organic matter sources and diagenesis in lake sediments. *Organic Geochemistry* **20**, 867-900.

Millar, C. I. *et al*., 2006. Late Holocene forest dynamics, volcanism, and climate change at Whitewing Mountain and San Joaquin Ridge, Mono County, Sierra Nevada, CA, USA. *Quaternary Research* **66**, 273-287.

Mote, P. W., *et al*., 2005. Declining mountain snowpack in western North America. *Bulletin of the American Meteorological Society* **86**, 39-49.

Nederbragt, 2004. *Digital sediment colour analysis as a method to obtain high resolution climate proxy records.* in Image Analysis, Sediments and Paleoenvironments. P. Francus ed. Kluwer Academic Publishers 105-124.

Regonda, S., M.P. Clark, B. Rajagopalan, and J. Pitlick, 2005: Seasonal cycle shifts in Hydroclimatology over the western United States. *Journal of Climate*, **18**, 372-384.

Roos, M., 1991: A Trend of Decreasing Snowmelt Runoff in Northern California. *Proc. 59th Western Snow Conference*, Juneau, AK, 29-36.

Roos, M., 1998, The Great New Year's Flood of 1997 in Northern California: Proc. Annual PACLIM Workshop, Pacific Grove, CA, Interagency Ecological Program Technical Report 57, 107-116.

Sachse, D. *et al*., 2006. δD values of individual n-alkanes from terrestrial plants along a climatic gradient—Implications for the sedimentary biomarker record. *Organic Geochemistry* **37**, 469-483.

Sachse, D. *et al*., 2004. Hydrogen isotope ratios of recent lacustrine sedimentary *n*-alkanes record modern climate variability. *Geochimica et Cosmochimica Acta* **68**, 4877-4889.

Sauer, P. E. *et al*., 2001. Compound-specific D/H ratios of lipid biomarkers from sediments as a proxy for environmental and climatic conditions. *Geochimica et Cosmochimica Acta* **65**, 213-222.

Schimmelman A. *et al*., 2006. Hydrogen isotopic (D/H) composition of organic material during diagenesis and thermal maturation. *Annual Review of Earth and Planetary Sciences* **34**, 501-533.

Seager, R., *et al*., 2008. Tropical Pacific forcing of North American medieval megadroughts: Testing the concept with an atmospheric model forced by coral-reconstructed SSTs. *Journal of Climate* **21**, 6175-6190.

Sessions, A. L. *et al*., 1999. Fractionation of hydrogen isotopes in lipid biosynthesis. *Organic Geochemistry* **30**, 1193-1200.

Sheldon, V. *et al*., 2004. A 300 year record of environmental change from Lake Tuborg, Ellesmere Island, Nunavut, Canada. *Journal of Paleolimnology* **32** 137-148.

Slack, J. R., and J. M. Landwehr, 1992. Hydro-Climatic Data Network (HCDN): A U.S. Geological Survey streamflow data set for the United States for the study of climate variations, 1874-1988. U.S. Geologic Survey Open-File Report 92-129, 193 pp.

Smith, G. I., *et al*., 1979. Areal distribution of deuterium in eastern California precipitation, 1968-1969. *Journal of Applied Meteorology* **18**, 172-188.

Stewart I. T., *et al*., 2005. Changes toward earlier streamflow timing across Western North America. *Journal of Climate* **18** 1136-1155.

Stine, S., 1994. Extreme and persistent drought in California and Patagonia during mediaeval time. *Nature* **369**, 546-549.

Woodhouse, C. A. and J. T. Overpeck, 2000. 2000 years of drought variability in the central United States. *Bulletin of the American Meteorological Society* **79,** 2693-2714.

Yang, H. and Y. Huang, 2003. Preservation of lipid hydrogen isotope ratios in Miocene lacustrine sediments and plant fossils at Clarkia, northern Idaho, USA. *Organic Geochemistry* **34**, 413-423.
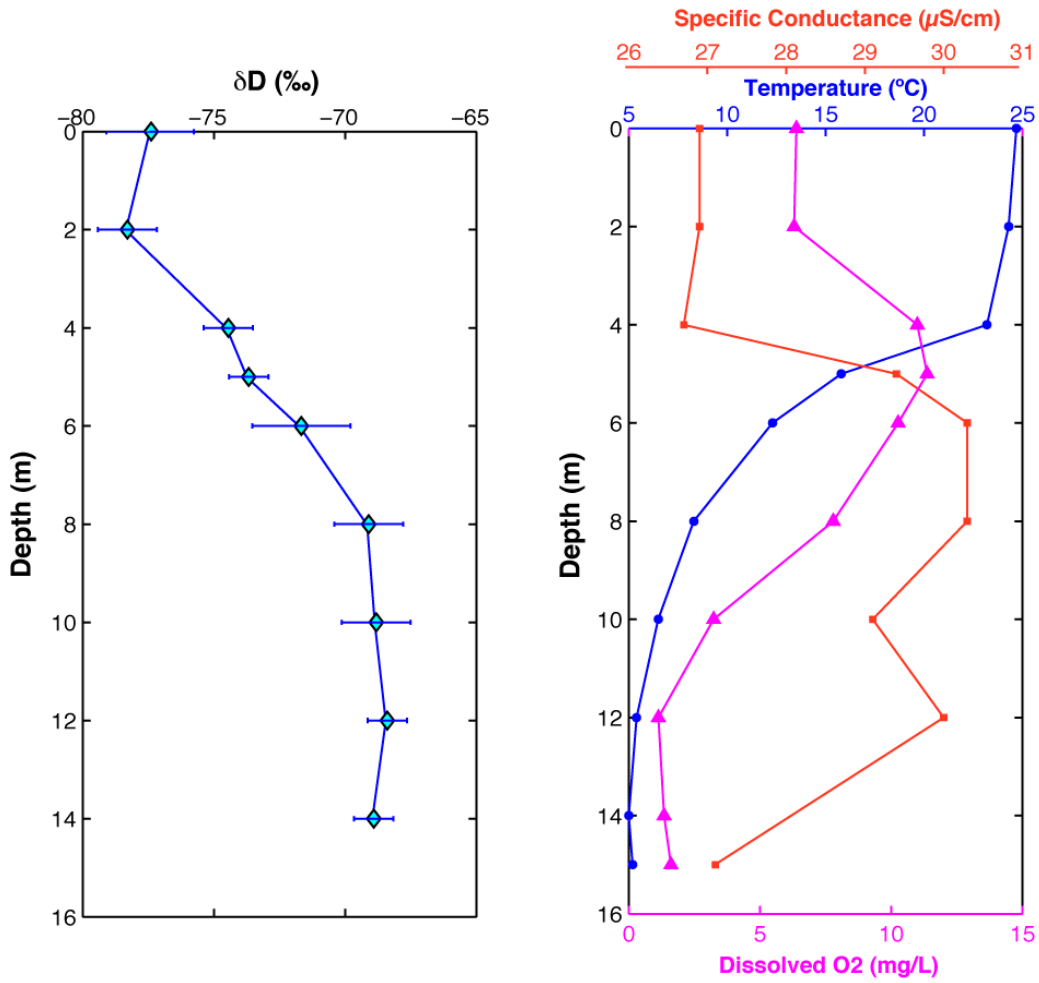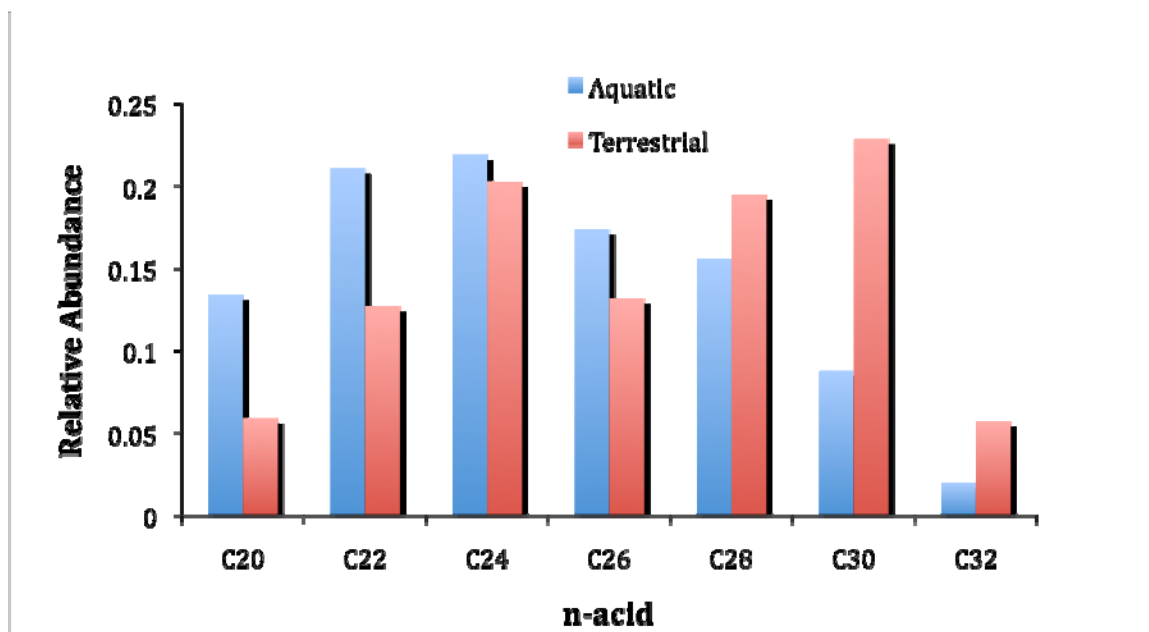
Figures
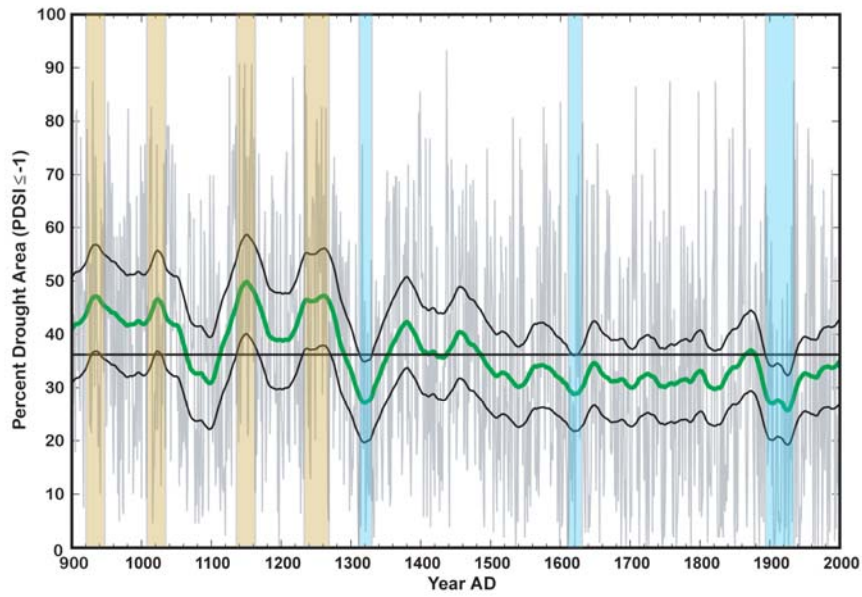
Figure 1 DAI time series created from 2.5º by 2.5º grid of PDSI reconstructions (Cook & Krusic, 2004). Green line is 60 year moving average and thin black lines are 95% bootstrap confidence interval. Straight black line is average for the entire period. Droughts, defined as intervals when the entire confidence interval is above the long term average are highlighted with brown bands while pluvials, where the opposite is true, are highlighted with blue bands.
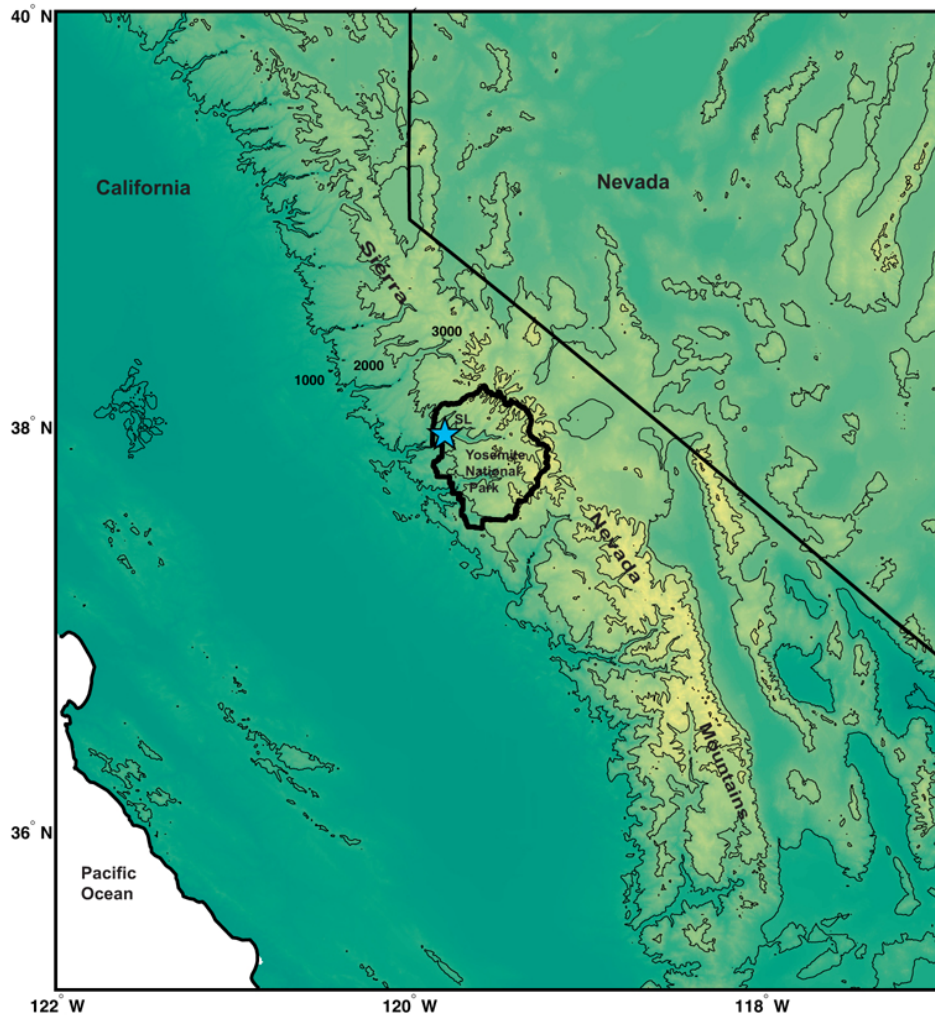
Figure 2 Location of Yosemite National Park along the crest of the Sierra Nevada Mountain Range. Swamp Lake is located in the northwest corner of the Park (indicated by blue star). Contours in meters.
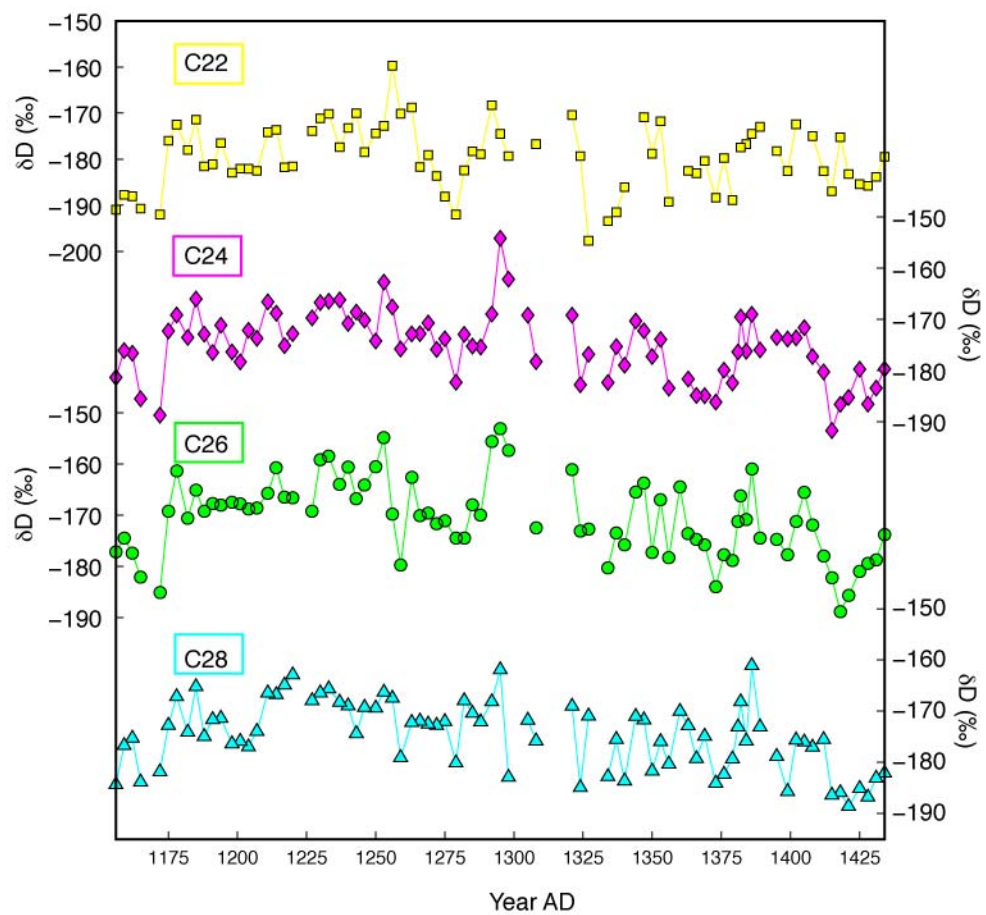
Figure 3. a) (left) δD profile from Swamp Lake, July 2009 **b)** (right) Temperature (blue), dissolved oxygen (pink) and conductivity (orange) profiles from Swamp Lake, July 2009.
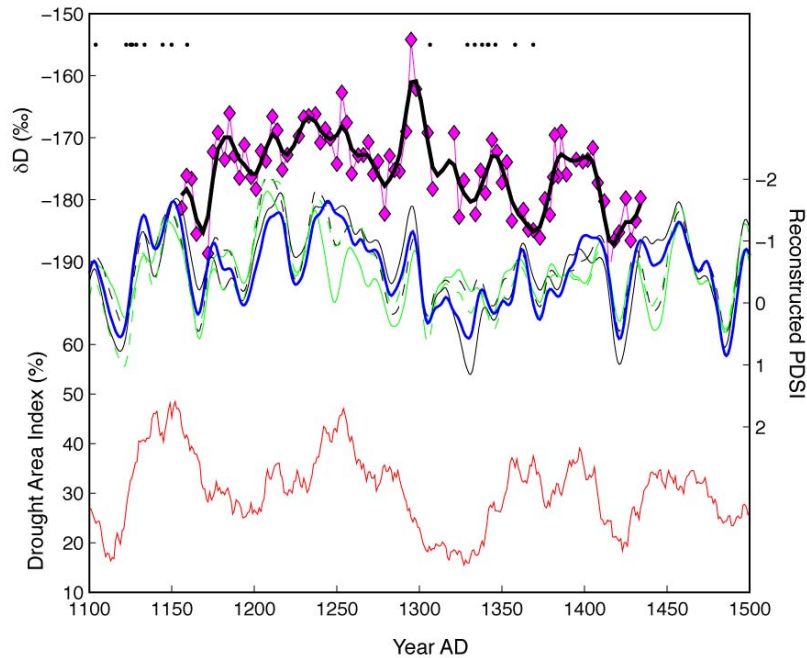
Figure 4. Average relative abundances of even numbered n-acids C20-C32 of aquatic (blue, N=5) and terrestrial (red, N=10) plants from Swamp Lake.
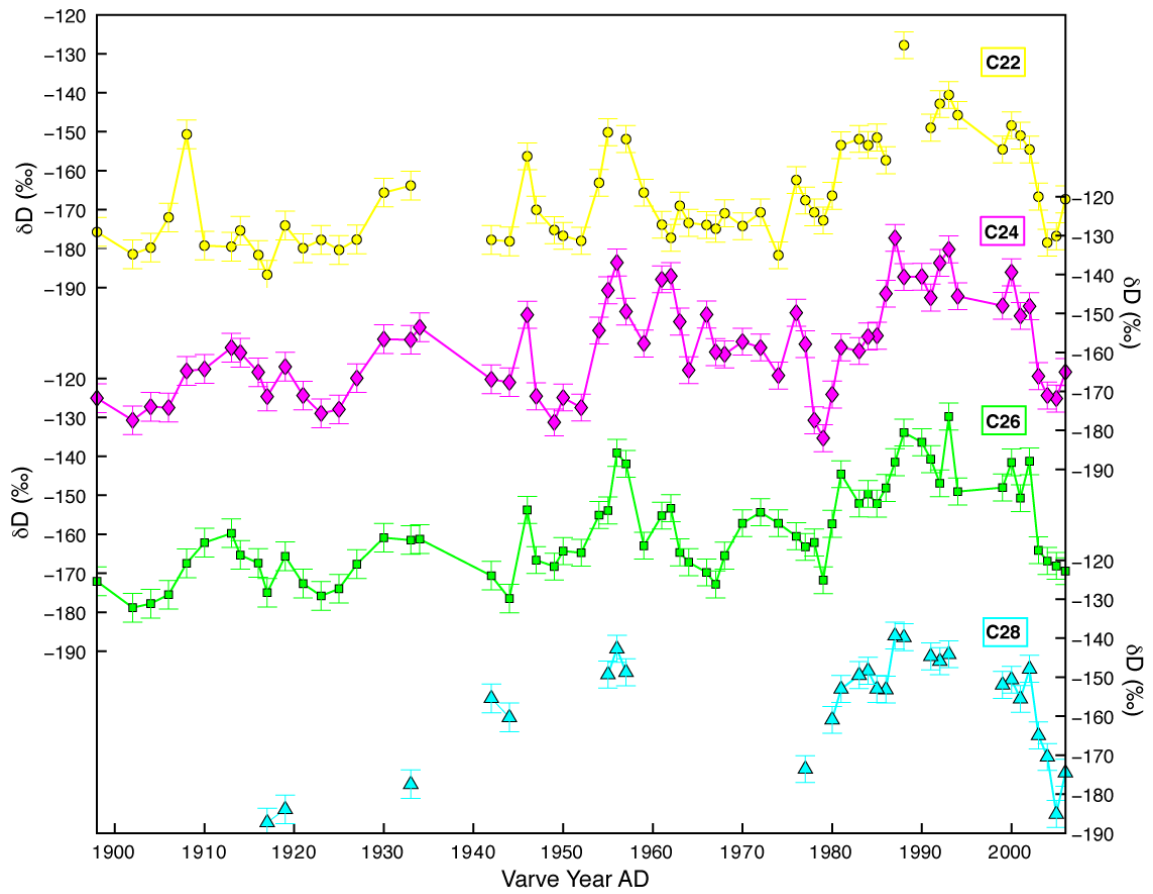
Figure 5. 20th century n-acid δD values even numbered C22-C28.

Figure 6. Medieval n-acid δD values even numbered C22-C28.

Figure 7. Comparison with C24 δD with death dates of sumberged tree stumps in the Sierra Nevada Mountains (Stine, 1994), reconstructed PDSI from of the closest grid squares in the North American Drought Atlas (Cook *et al*., 2008) and Drought Area Index (Cook *et al*., 2004). Death dates: black dots, raw C24: pink diamonds, smoothed C24 with smoothing spline: thick black line, reconstructed PSDI: blue, green and thin black solid and dashed lines, Drought Area Index: red line.

Table 1. List of Vegetation Species Sampled			
Species	Vegetation Type	Common Name	Location
Dulichium arundinaceum	sedge grass	threeway sedge	shallows, west bank
Carex lenticularis	sedge grass	lakeshore sedge	west bank
Carex utriculata	sedge grass	beaked sedge	west bank
Ceanothus integerrimus	shrub	deer brush	~10m from west bank
Arctostaphylos viscida	shrub	white manzanita	~7m from west bank
Alnus rhombifolia	tree	white alder	growing on west bank
Rhodoendron occidentale	shrub	western azalea	~10m from west bank
Menyathes trifoliata	emergent aquatic	bog bean	shallows, west bank
Quercus kelloggii	tree	black oak	growing on west bank
Pinus ponderosa	tree	ponderosa pine	~40m from west bank
Calcoedrus deccurrens	tree	insense cedar	~40m from west bank
Brasenia schreberi	emergent aquatic	watershield	shallows, west bank
Schoenoplectus subterminalis	submergent aquatic	swaying bulrush	shallows
Potamogeton robbinsii	submergent aquatic	Robbin's pondweed	shallows
Pseudotsuga menziesii	tree	douglas fir	~40m from west bank
Nuphar polysepala	emergent aquatic	water lily	shallows, north

Table 2. Correlation of 20th century C24 *n*-acid dD with Instrumental Climate Records[a]	
Climate Record	Correlation Coefficient, r with C24 n-acid dD[c]
Hetch Hetchy (HTH) annual average precipitation (1910-2006)	-0.24
California Climate Division 5 annual average precipitation (1898-2006)	**-0.32**
Bee Hive Meadows (BHV) April 1 SWE (1932-2006)	**-0.43**
Donner Summit (DNS) April 1 SWE (1910-2006)	-0.26
California Climate Division 5 PDSI (1898-2006)	**-0.31**
Tree-ring Reconstructed PDSI from Grid Square 47 (1898-2006)[b]	-0.21

[a] All instrumental records 2 year running mean

[b] from Cook *et al*., 2008.

[c] r values in bold significant at the 95% confidence interval